THE ROYAL SOCIETY
PUBLISHING

Climate-driven benthic invertebrate activity and biogeochemical functioning across the Barents Sea polar front

Martin Solan[1], Ellie R. Ward[1], Christina L. Wood[1], Adam J. Reed[1], Laura J. Grange[2] and Jasmin A. Godbold[1]

[1]School of Ocean and Earth Science, National Oceanography Centre Southampton, University of Southampton, Waterfront Campus, European Way, Southampton SO14 3ZH, UK
[2]School of Ocean Sciences, Bangor University, Bangor, Gwynedd LL57 2DG, UK

MS, 0000-0001-9924-5574

Arctic marine ecosystems are undergoing rapid correction in response to multiple expressions of climate change, but the consequences of altered biodiversity for the sequestration, transformation and storage of nutrients are poorly constrained. Here, we determine the bioturbation activity of sediment-dwelling invertebrate communities over two consecutive summers that contrasted in sea-ice extent along a transect intersecting the polar front. We find a clear separation in community composition at the polar front that marks a transition in the type and amount of bioturbation activity, and associated nutrient concentrations, sufficient to distinguish a southern high from a northern low. While patterns in community structure reflect proximity to arctic versus boreal conditions, our observations strongly suggest that faunal activity is moderated by seasonal variations in sea ice extent that influence food supply to the benthos. Our observations help visualize how a climate-driven reorganization of the Barents Sea benthic ecosystem may be expressed, and emphasize the rapidity with which an entire region could experience a functional transformation. As strong benthic-pelagic coupling is typical across most parts of the Arctic shelf, the response of these ecosystems to

a changing climate will have important ramifications for ecosystem functioning and the trophic structure of the entire food web.

This article is part of the theme issue 'The changing Arctic Ocean: consequences for biological communities, biogeochemical processes and ecosystem functioning'.

1. Introduction

The Arctic Ocean seafloor hosts a diverse and productive benthic ecosystem that forms an important component of an intimately coupled benthic-pelagic system [1], but the structure and functioning of this compartment is rapidly and disproportionately being modified by climate change [2–5]. Multiple, simultaneously occurring, system responses to climatic forcing challenge species physiologically, leading to alterations in the diversity, composition [6,7] and trophic structure of assemblages [8], as well as feedbacks that moderate associated ecosystem process rates [9,10]. In the high Arctic, deterioration in the extent and thickness of sea ice results in a series of cascading changes (light, temperature, nutrients, sea-ice edge mixing, season extension) that influence surface primary productivity [11], the supply of organic matter to the sea floor [12,13], and the structure of recipient microbial [14] and invertebrate [15–17] communities that regulate carbon and nutrient cycles [18,19]. At the same time, physical changes are causing a weakening of water column stratification such that the Arctic ocean is becoming a more Atlantic influenced system [20,21], with repercussions for the entire marine food web [22–24]. While the retraction of ice northwards results in a well-known poleward shift in species distribution [25–27], and much is known about the functional role of boreal and arctic benthic fauna [28–30], uncertainties remain about how concurrent adjustments in biodiversity and food supply affect benthic biogeochemical responses. One source of ambiguity is that changes in sea ice extent, and all of its correlates, exhibit considerable inter-annual variability [31,32] that can appear to manifest as alternative ecosystem responses [33], making it difficult to distinguish natural variability within a period of gradual change from the onset of an abrupt regime shift [34]. Furthermore, the transition or borealization of arctic fauna [35] can positively affect local levels of biodiversity [36,37] and/or provide a functional buffer by maintaining ecological processes [38], depending on local context [39,40] and how post-borealization species interactions and compensatory responses are realized [41,42].

The net effect that faunal responses to a changing Arctic will have on biogeochemical cycles is difficult to anticipate [43], but it is clear that climate-driven variation in the functional attributes of sediment communities will have a significant role in incorporating recently deposited and readily degradable organic matter into the sediment profile [13,44,45]. Indeed, the particle reworking and ventilatory behaviour (= bioturbation) of invertebrates can fundamentally change sediment biogeochemistry [46,47], including organic matter mineralization, oxygen, nutrient and sulfur cycling as well as mineralization processes, such as shell dissolution or iron and manganese reduction. Consequently, the extent of faunal reworking influences whether organic material is preserved through burial [48] or recycled via various pathways of mineralization [49] which, in turn, replenish bottom waters [50,51]. With movement of the Polar Front and marginal ice further north, the supply of labile material to the sediment surface is likely to increase and move polewards under an open ocean (in contrast to other polar regions, where organic matter builds up at the seafloor due to low seafloor temperatures, e.g. western Antarctic Peninsula [52]), but the macromolecular composition of surface sediments will be distinguishable [53]. Nevertheless, and despite cold temperatures, faunal utilization and incorporation of organic matter into the sediment profile appears to be rapid, albeit species-specific [13], and active deep mixing tends to be more important than sedimentation in capturing the organic matter resource [54]. These coupled biological and biogeochemical processes are crucial for benthic-pelagic coupling and ecosystem productivity, as well as the long-term removal of carbon from the ocean-atmosphere system [55]. However, most studies of Arctic benthic biodiversity have

been restricted to the classification of assemblage structure and do not include biogeochemical flux analyses [56–58], while attempts to explain variation in benthic biogeochemistry have not explicitly considered bioturbation as a causative factor [59]. Moreover, although the distribution of functionally important species traits has received some attention [29,30], there are few direct measurements of faunal activity [54,60–65] and no regional-scale assessments of the faunal mediation of biogeochemistry. Hence, the objective of this study was to quantify the effect of changing sea ice cover on benthic invertebrate biodiversity and explore how changes in environmental setting and assemblage composition may affect sediment mixing and associated levels of nutrient concentration across a sea ice transect that intersects both the oceanographic [66] and benthic [56] polar front. We anticipated that differences in faunal composition between northern (Arctic) and southern (Atlantic) assemblages would lead to contrasts in bioturbation and nutrient concentrations [47], and hypothesized that maximal faunal activity would coincide with the approximate position of the polar front due to the stimulatory effects of turbulent mixing and nutrient advection [67]. We expected that this spatial division would reflect a contrast in the source, quantity and/or reactivity of sediment organic matter, but further hypothesized that inter-annual variation in conditions at specific locations along the sea ice gradient would modify the community response. Returning these outcomes will emphasize the importance of timing and context in moderating how benthic environments respond to external forcing, and highlight the need to incorporate such complexities into current thinking [43,55] and expectation [68].

2. Material and methods

(a) Study location

To quantify the effect of changing sea ice cover on benthic invertebrate biodiversity and faunal mediation of nutrient concentrations (ecosystem functioning, defined here as the nutrient pool resulting from the interactions between a biotic assemblage and its abiotic environment), we investigated the marginal areas of the Eurasian Arctic Ocean southeast to northeast of Svalbard. Within this area, the Barents Sea is experiencing an acceleration in warming and weakening of water column stratification that effects the annual extent of sea ice (see electronic supplementary material, figure S1) and position of the polar front [21]. Data were collected during two consecutive summer cruises (*RRS James Clark Ross*: JR16006, 30th June to 8th August 2017; JR17007: 10th July to 5th August 2018) following a transect along the 30°E meridian (Stations B13-B17 and Xs; see electronic supplementary material, table S1) that intersects both the oceanographic [66] and benthic [56] polar front (see electronic supplementary material, figure S2). To minimize the effect of non-climatic drivers of change, stations were selected with comparable water depths (200–400 m), sediment type and bottom fishing activity [69,70]. Bottom fishing activity was minimized by selecting locations that showed low levels of activity (based on VMS tracking data, visualized at: https://kart.barentswatch.no/) and we verified that there was no recent activity at the point of station occupancy using sediment surface imagery [71] and geochemical profiles [72,73].

(b) Experimental set-up and design

At each station four replicate intact sediment cores (LWH: $20 \times 20 \times 12$ cm) were obtained from replicate 0.1 m^2 USNL (Unites States Naval Laboratory) box cores using a core extruder (see electronic supplementary material, figure S3), transferred to transparent acrylic aquaria (internal dimensions, LWH: $20 \times 20 \times 34$ cm) and overlain with approximately 8 l (20 cm depth) surface seawater (salinity, approx. 34). Aquaria (2017, $n = 20$; 2018, $n = 24$) were randomly transferred to one of two insulated fibreglass seawater baths (LWH: $1.2 \times 1.2 \times 0.8$ m, Tanks Direct, UK; see electronic supplementary material, figure S4) and maintained at a representative ambient bottom temperature (see electronic supplementary material, table S2, $1.5 \pm 0.5°C$; Titan 1500 chiller unit, AquaMedic) in the dark. Each aquarium was continually aerated by bubbling through a glass

pipette and supplied approximately 0.03 g of flaked fish food aquarium^{-1} (Aquarian Tropical Flake) on alternate days. To avoid excessive accumulation of nutrients and metabolites associated with the assembly process, a partial (80%) seawater change on each aquarium was performed after 24 h. Aquaria were incubated for 12 days.

Sediment particle size frequency distributions from the USNL box cores were determined optically using a Malvern Mastersizer 2000 He-Ne LASER diffraction sizer at the Department of Geography, University of Cambridge following standard protocols (available at: http://www.geog.cam.ac.uk/facilities/laboratories/techniques/) and were used to resolve mean particle size, sorting, skewness and kurtosis [74] using GRADISTAT [75]. Loss on ignition was used to determine sediment organic material content (%). Further characterization of sediment organic matter processing and total organic carbon were beyond the scope of this contribution, but are provided by Freitas *et al.* [72] and Stevenson *et al.* [73].

(c) Measurements of faunal activity

Faunal mediated sediment particle reworking was estimated by establishing the redistribution of optically distinct particulate tracers (luminophores: 215 g aquaria^{-1}, fluorescent green, less than 200 µm silica sand, density 2.35 kg dm^{-3}; Glass Pebbles Ltd., UK). Luminophores were evenly distributed across the sediment surface (see electronic supplementary material, figure S3) immediately after the partial seawater change. After 12 days, the redistribution of luminophores was quantified from stitched composite images (RGB colour, JPEG compression; see electronic supplementary material, figures S5 –S10) of all four sides of each aquarium taken using a digital SLR camera (Canon 400D: 2017, 10 s exposure, f5.6 aperture, ISO 400, 83 µm pixel^{-1}; 2018, 10 s exposure, f5.6 aperture, ISO 800, 74 µm pixel^{-1}) housed within a UV illuminated imaging box (f-SPI, [76,77]). The mean ($^{f-SPI}L_{mean}$, time-dependent indication of short term faunal mixing) and maximum ($^{f-SPI}L_{max}$, maximum vertical extent of faunal mixing) mixed depth of particle distribution were calculated from extracted profile data (see electronic supplementary material, figures S11–S12) using a custom-made semi-automated macro that runs in *ImageJ* (v. 1.47 s, released 3rd June 2013), a java-based public domain program developed at the US National Institutes of Health (http://rsb.info.nih.gov/ij/index.html). For comparative purposes [78], we also estimated the biodiffusion coefficient (Db, cm^2 year^{-1}; [79]) that describes the rate at which the variance of the location of a particle tracer (i.e. the spread) changes over time within the sediment profile, providing a descriptor of bioturbation intensity. Surface reworking activity was estimated by calculating the maximum vertical deviation of the sediment-water interface (upper–lower limit = surface boundary roughness, SBR).

The ventilatory behaviour of the infauna (hereafter, bioirrigation) was estimated from absolute changes in the concentration (10 mM, 8.231 g NaBr dissolved in seawater aquarium^{-1}) of the inert tracer sodium bromide (Δ [Br$^-$], mg l^{-1}; negative values indicated increased infaunal ventilatory activity, [80]) over an 8 h period on day 12, determined using a Tecator flow injection auto-analyser (FIA Star 5010 series).

(d) Measurements of ecosystem function

Accumulated water column concentrations (µmol l^{-1}) of NH$_4$-N, NO$_x$-N (i.e. NO$_3$-N + NO$_2$-N) and PO$_4$-P were determined after 12 days incubation from standardized samples (taken from the centre of each aquarium at approx. 5 cm depth, 0.45 µm NALGENE filtered) following standard protocols using a Lachat Quikchem 8500 flow-injection auto-analyser.

(e) Identification of fauna

The macrofauna retained (500 µm sieved) from each aquarium were fixed in 10% phosphate-buffered formalin (4% formaldehyde) and stored in sealed plastic buckets for a minimum of three months [81]. Prior to identification samples were rinsed and preserved in 70% industrial

methylated spirit (IMS). All individuals were identified to the lowest possible taxon with abundance and biomass per taxon noted. Biomass was obtained using blotted wet weight (± 0.0001 g). All molluscs were weighed inclusive of shells, tube-dwelling polychaetes were weighed without tubes, and sediment was removed from the body cavity of specimens of *Ctenodiscus crispatus* prior to weighing.

(f) Statistical analyses

Analysis of variance (ANOVA) models were developed to investigate the effects of station location (5 levels: B13-B17) and year (2 levels: 2017, 2018), and their interaction, on infaunal sediment particle reworking (SBR, $^{f-SPI}L_{med}$, $^{f-SPI}L_{mean,}$ $^{f-SPI}L_{max}$), burrow ventilation ($\Delta[Br^-]$) and nutrient concentration ($[NH_4 - N], [NO_x - N]$, $[PO_4 - P]$). Data from station Xs is presented for comparative purposes, but were not included in any statistical analysis as data were not available for both years. Model assumptions (homogeneity of variance, normality, presence of influential outliers) were assessed using plots of residuals versus fitted values, Q-Q plots and Cook's distance [82]. Where data exploration identified a violation of homogeneity of variance, data were analysed using a *varIdent* variance-covariate structure and generalized least-squares (GLS) estimation [83,84] to allow the residual spread to vary with individual explanatory variables. The optimal variance–covariate structure was determined using restricted maximum-likelihood (REML) estimation by comparing the initial ANOVA model without variance structure to the equivalent GLS model incorporating specific variance structures using AIC and visualization of model residuals. The optimal fixed structure was determined by applying backward selection using the likelihood ratio test with maximum-likelihood (ML) estimation [82,84,85].

The single and interactive effects of station and year on macrofaunal community composition were visualized using non-metric multi-dimensional scaling (nMDS) based, first, on the abundance (square-root transformed), and, second, on the biomass of taxa, to identify any transition in faunal assemblage structure across the polar front. Community differences associated with station (B13–B17) and/or year (2017, 2018) were determined using a permutational multivariate analysis of variance (PERMANOVA, [86]) with 999 iterations. The relative contribution of individual taxa to the dissimilarity between samples was identified using similarity percentages (SIMPER, [87]) based on square-root transformed abundance or biomass. As joint species absences provide important discriminatory information for treatment effects, data were zero adjusted by adding a dummy variable (abundance, 1; biomass, 0.0001; [88]).

All analyses were performed in R [89] using the *nlme* (ANOVA and GLS analyses; [90]) and *vegan* (nMDS, PERMANOVA and SIMPER analyses; [91]) packages.

3. Results

(a) Sediment and faunal composition

Sediment particle size distributions (see electronic supplementary material, figures S13–S14) showed no notable patterns between stations and/or across years, and largely consisted of poorly sorted symmetrical mesokurtic fine to medium silts (approx. 90% less than 63 µm) with an organic material content of approximately 6–8% (see electronic supplementary material, table S3).

A total of 2550 faunal individuals representing 153 taxa were recovered from stations B13-B17, with 1353 individuals (22.8602 g biomass) representing 123 taxa in 2017 and 1197 individuals (15.8390 g biomass) representing 113 taxa in 2018. An additional 403 individuals (4.3943 g biomass), representing 45 taxa, were recovered from station Xs in 2018. A total of 157 unique taxa (63% identified to species level, 92% to genus level; 2953 individuals, 43.0935 g biomass) were recovered across all stations and both years. Species richness (number of species), evenness, total abundance, and total biomass for all stations and years are presented in electronic supplementary material, table S4. We observed a distinct separation in macrofaunal community
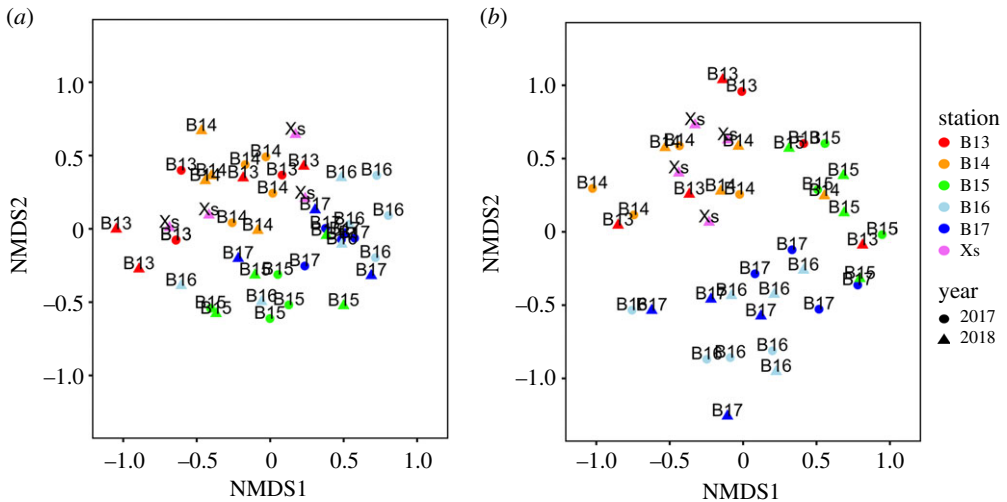
Figure 1. Classification of the faunal assemblages in the Barents Sea reveal a clear separation between northern and southern stations. Non-metric two-dimensional (nMDS) representations of Bray–Curtis similarity matrices are presented based on (*a*) square root transformed abundance and (*b*) untransformed biomass for stations B13–B17 (indicated by colour) in 2017 (circles) and stations B13–B17 and Xs in 2018 (triangles). Ordination diagnostics are presented in electronic supplementary material, figure S15. Dimensionality representation stress values ($k = 3$) are (*a*) 0.163 and (*b*) 0.143. (Online version in colour.)

structure based on both abundance (PERMANOVA: station, $F = 5.526$, d.f. $= 5$, $p < 0.001$; year, $F = 2.046$, d.f. $= 1$, $p < 0.001$; figure 1*a*; electronic supplementary material, figure S15a,c,e) and biomass (PERMANOVA: station $\times$ year, $F = 1.427$, d.f. $= 4$, $p = 0.032$; figure 1*b*; electronic supplementary material, figure S15b,d,f). SIMPER analysis indicated that approximately half of the dissimilarity in assemblage composition between years was associated with 16 taxa when based on abundance ($\sum S_i = 50.94\%$, *Spiochaetopterus typicus*, *Maldane sarsi*, Yoldiidae, *Nephasoma procera*, *Spiophanes kroyeri*, *Adontorhina* juv., *Lumbrineris mixochaeta*, Nematoda, *Leitoscoloplos mammosus*, *Chaetozone setosa*, *Mediomastus fragilis*, *Haploops tubicola*, *Chirimia biceps*, *Ophelina abranchiata*, *Levinsenia gracilis*, Nemertea) and 5 species when based on biomass ($\sum S_i = 52.99\%$, *Ctenodiscus crispatus*, *Spiochaetopterus typicus*, *Astarte crenata* agg., *Maldane sarsi*, *Chirimia biceps*). Approximately half of overall dissimilarity ($\sum S_i \sim 50\%$) between stations was typically associated with 11–17 taxa when based on abundance and 3–7 taxa when based on biomass (see electronic supplementary material, table S5). In general, taxa such as *Spiochaetopterus typicus*, *Spiophanes kroyeri*, *Maldane sarsi* and the Yoldiidae were important numerically, while taxa such as *Spiochaetopterus typicus*, *Ctenodiscus crispatus*, *Aglaophamus malmgreni* and *Astarte sulcata* were important in terms of biomass. However, the identity and rank importance of taxa contributing most to overall community similarity/dissimilarity was not uniformly expressed, and contrasted between the southern and northern stations.

(b) Effects on faunal activity

Surface boundary roughness differed between years (*L*-ratio $= 3.769$, d.f. $= 1$, $p < 0.0001$), but not between stations (*L*-ratio $= 6.106$, d.f. 4, $p = 0.1914$), and was not dependent on their interaction (station $\times$ year: *L*-ratio $= 3.008$, d.f. $= 4$, $p = 0.5564$). Overall, there was evidence of a decreasing SBR with increasing latitude and lower mean SBR ($\pm$s.d., $n = 20$) in 2017 (1.050 ± 0.366 cm) relative to 2018 (1.831 ± 0.713 cm) (figure 2*a*). The mean mixed depth of particle redistribution ($^{f-SPI}L_{mean}$) differed between years (*L*-ratio $= 8.201$, d.f. $= 1$, $p < 0.01$) and across stations (*L*-ratio $= 25.337$, d.f. $= 4$, $p < 0.0001$), but there was no interaction between station and year (station $\times$ year: *L*-ratio $= 4.057$, d.f. $= 4$, $p = 0.3984$). Overall, mean $^{f-SPI}L_{mean}$ ($\pm$s.d., $n = 20$)
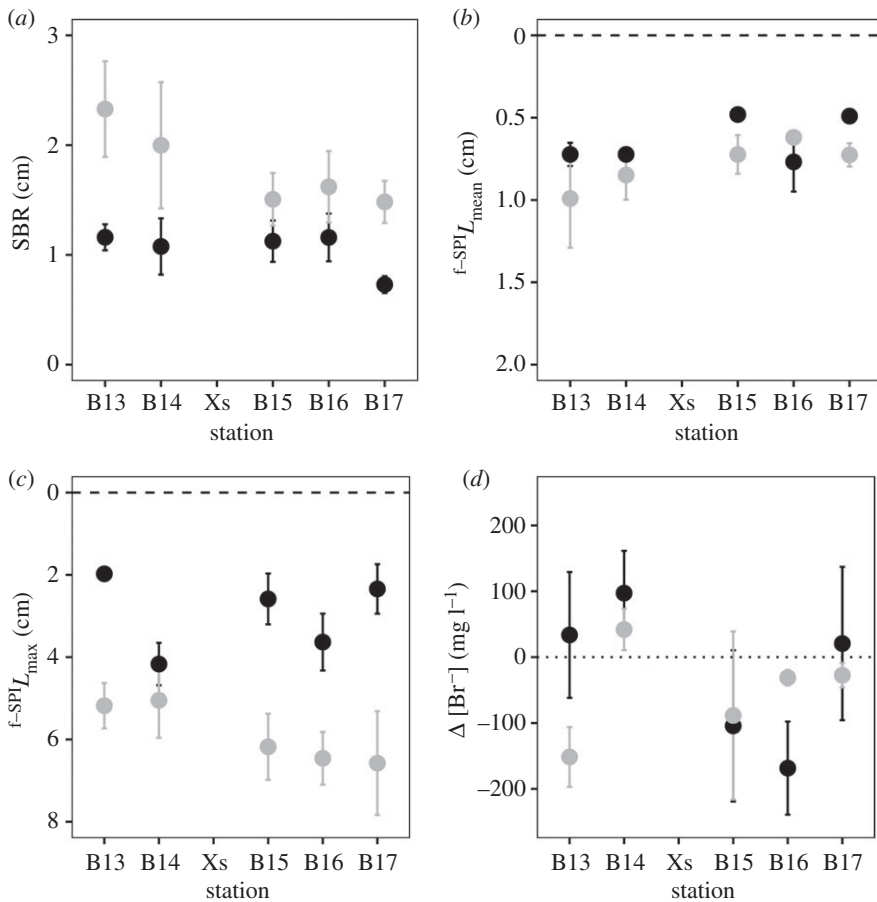
Figure 2. The effects of station and year on mean ($\pm$s.e., $n = 4$) bioturbation activity as indicated by (*a*) surface boundary roughness, (*b*) mean mixed depth, $^{f-SPI}L_{mean}$, (*c*) maximum mixed depth, $^{f-SPI}L_{max}$ and (*d*) ventilatory behaviour, Δ [Br$^-$] for stations B13–B17 in 2017 (black) and stations B13–B17 and Xs in 2018 (grey). For Δ [Br$^-$], negative values indicate increased bioirrigation. In panels (*b*) and (*c*), dashed lines indicate the position of the sediment-water interface. In panel (*d*), the dotted line indicates no change in [Br$^-$]. Sediment profile images and associated luminophore distribution profiles are presented in electronic supplementary material, figures S5–S12.

was shallower in 2017 (0.6371 ± 0.2016 cm) relative to 2018 (0.7817 ± 0.3160 cm) and, although insignificant, showed evidence of shallowing with increasing latitude (from 0.8568 ± 0.4271 cm at B13 to 0.6082 ± 0.156 cm at B17, $n = 8$; figure 2*b*). The maximum mixed depth of particle redistribution ($^{f-SPI}L_{max}$) differed between years ($F_{1,30} = 41.0906$, $p < 0.0001$) but not with station ($F_{4,30} = 1.0784$, $p = 0.3846$) or their interaction (station $\times$ year: $F_{4,30} = 1.5187$, $p = 0.2218$). Mean $^{f-SPI}L_{max}$ ($\pm$s.d., $n = 20$) was shallower in 2017 (2.9407 ± 1.2900 cm) relative to 2018 (5.8874 ± 1.6816 cm), and ranged from 1.9751 ± 0.2347 cm at B13 to 4.1672 ± 1.0326 cm at B14 in 2017, exhibiting a step change of approximately 1.57 cm between the southern (B13 and B14, $n = 8$, 4.8734 ± 1.3973 cm) and northern (Xs, B15-B17, $n = 12$, 6.4403 ± 1.6234 cm) stations (figure 2*c*). Bioirrigation behaviour was independent of year and/or station (intercept only model), but absolute values indicated higher activity at stations furthest away from the polar front and in 2018 (figure 2*d*).

The redistribution of luminophores approximated a biodiffusive profile, with mean ($\pm$SD, $n = 4$) station Db values ranging from 1.922 ± 0.208–6.089 ± 2.324 cm^2 year^{-1} in 2017 and from 2.550 ± 0.573–16.700 ± 15.497 cm^2 year^{-1} in 2018 (see electronic supplementary material, table S6).
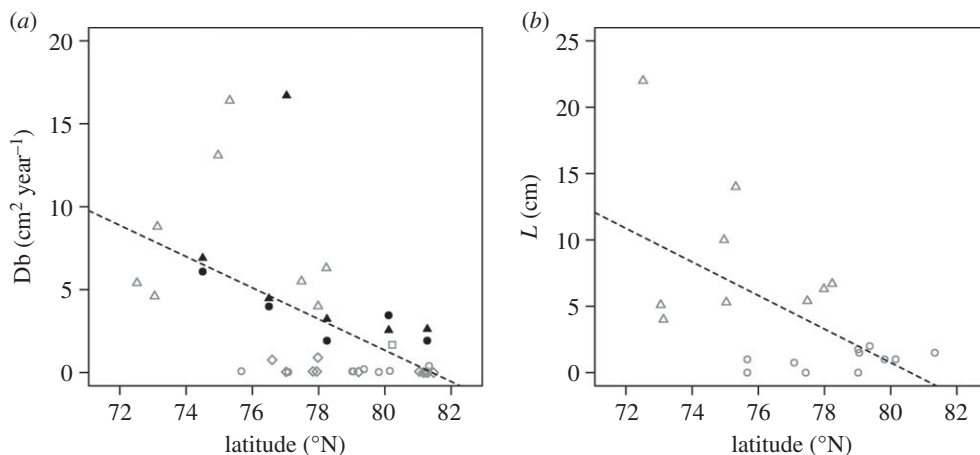
Figure 3. The relationship between (*a*) the bioturbation coefficient, Db, and (*b*) the mixed depth, *L*, and latitude for the Barents Sea shelf region. Data are presented from both the present (2017, black closed circles; 2018, black closed triangles) and previous studies (grey, source indicated by open circle [60], triangle [61], square [62] or diamond [64]). Dashed lines represent linear regression of the pooled data: (*a*) slope $= -0.942$, intercept at $71.5°$ N $= 9.346$, $F = 16.26$, $p < 0.001$, and (*b*) slope $= -1.265$, intercept at $71.5°$ N $= 13.749$, $F = 9.169$, $p < 0.01$.

Comparison of Db values across our transect showed a trend of declining bioturbation activity with latitude, consistent with previous findings [78] for Db and *L* in the Barents Sea region (figure 3). A single individual of *Quasimelita quadrispinosa* (Station Xs, replicate 1, see electronic supplementary material, figure S16) formed extensive galleries and mounding, and made disproportionate contributions to community bioturbation (as seen across all bioturbation metrics for this station, figure 2).

The amount of sediment organic material was dependent on the interactive effects of station and year (station × year: $F = 1.52$, d.f. $= 4$, $p = 0.451$), and indicated that, with the exception of station B13, organic material was higher in 2017 relative to what it was in 2018 (see electronic supplementary material, table S3 and figure S17). Mean ($\pm$s.d., $n = 4$). Organic material values were higher in the southern most station (B13: 2017, $6.74 \pm 0.40\%$; 2018, $6.76 \pm 0.15\%$) and peaked at station B14 (2017, $8.078 \pm 0.30\%$; 2018, $7.47 \pm 0.26\%$), but declined to the north (approx. 6–7%). Station Xs in 2018 showed much lower mean organic material ($4.58 \pm 0.38\%$) values relative to the other stations. With the exception of $^{f-SPI}L_{max}$ across all stations in 2017 (Spearman correlation: $\rho = 0.621$, d.f. $= 20$, $p < 0.01$), none of our bioturbation metrics were associated with sediment organic material.

(c) Effects on ecosystem functioning

[NH$_4$-N] depended on the interaction between station and year (station × year: L-ratio $= 10.943$, d.f. $= 4$, $p < 0.05$). With the exception of station B13, [NH$_4$-N] was lower at each station in 2017 in comparison to 2018. Irrespective of year, mean ($\pm$s.d., $n = 8$) [NH$_4$-N] was highest at stations B14 (7.508 ± 2.459 µmol l^{-1}) and Xs (7.965 ± 2.698 µmol l^{-1}), and lowest at station B15 (2.034 ± 0.881 µmol l^{-1}) (figure 4*a*). [NO$_x$-N] differed between stations (L-ratio $= 30.568$, d.f. $= 8$, $p < 0.0001$), but not between years (L-ratio $= 5.050$, d.f. $= 5$, $p = 0.4098$) or their interaction (station × year: L-ratio $= 5.049$, d.f. $= 4$, $p = 0.2823$), and increased in concentration with latitude from less than 2 µmol l^{-1} south of the polar front to 4.968 µmol l^{-1} at station B17 (figure 4*b*). [PO$_4$-P] was dependent on the interactive effects of station and year (station × year: L-ratio $= 13.436$, d.f. $= 4$, $p < 0.01$), and indicated that, with the exception of station B13, [PO$_4$-P] was much lower in 2017 relative to what it was in 2018 (figure 4*c*).
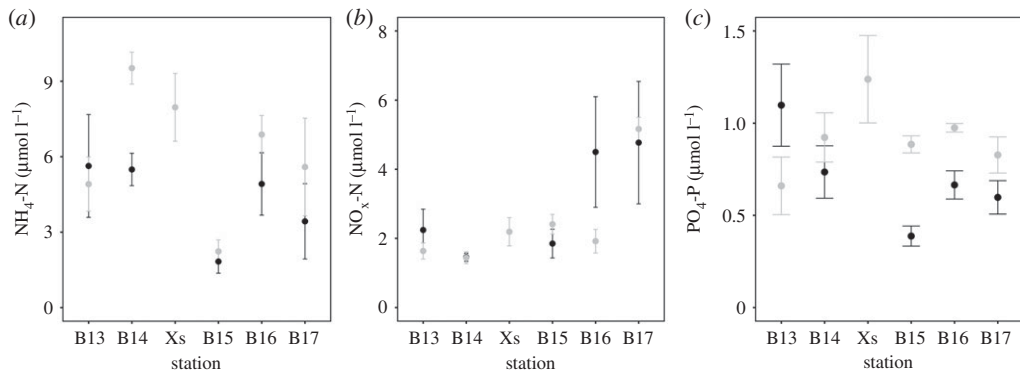
Figure 4. The effects of station and year on mean ($\pm$s.e., $n = 4$) nutrient concentrations as indicated by (a) [NH$_4$-N], (b) [NO$_x$-N] and (c) [PO$_4$-P] for stations B13–B17 in 2017 (black) and stations B13–B17 and Xs in 2018 (grey).

4. Discussion

Changes in the structure and composition of the Arctic biome under rapid climate warming continue to be observed [38,56], most prominently expressed as range shifts toward higher latitudes [25–27,34] and compositional change in favour of species adapted to higher temperatures (e.g. Atlantification of the high Arctic) [20,21,35]. Given the causal link between biodiversity and many ecosystem properties [92], concern is mounting that concomitant changes in ecosystem functioning are taking place that, in the longer term, could be sufficient to force a regime shift and/or cause an abrupt change in functioning [34,93]. Difficulties are emerging with this narrative, however, because multiple interacting factors modify biodiversity-function relations [94] and community responses [41], and local variations in how drivers of change are expressed and are received (including lags) can override trends associated with macro-climatic forcing [39,95]. In addition, evidence is emerging that long-term resilience depends on the nature of covariation between multiple components of stability [96], which are seldom incorporated in empirical investigations. The role of water mass inertia in buffering the extent and rate of benthic faunal change following sea ice reduction, for example, is unknown. Here, we find strong evidence that changes in environmental setting related to inter-annual variations in sea ice alter the benthic community response from seasonal or latitudinal expectation; that is, the expression of climate forcing at the benthos (here, approx. 300 m water depth) is not temporally or spatially homogeneous [97,98] and leads to context-specific changes in species behaviour and related levels of ecosystem functioning [40,99]. At the same time, our analysis confirms the presence of distinct basal infaunal communities and a faunal separation between northern (Arctic) and southern (Atlantic) assemblages at a latitude that corresponds with the operational oceanographic [66] and benthic [56] polar front. By extension, when taken together, our findings give credence to the view that Arctic dwelling benthic assemblages are more robust than physiological assessments may indicate [100], and it is tempting to speculate that a proportion of the community are adapted to maximize seasonal shifts in, for example, resource availability [101]. However, as has been highlighted before [28], detection of the influence of environmental conditions on the structure and function of benthic communities requires an overview of how functionally relevant infaunal traits covary with changing abiotic and biotic circumstance [102], and how species interactions and ecological roles vary with context [103].

Although the position of the polar front [104,105] and the conditions that influence it [20] are still poorly defined, there is evidence that warming is leading to changes in its intensity [20,106]. Atlantic surface waters are heating up at approximately 0.4°C decade^{-1}, and Arctic waters at approximately 0.6°C decade^{-1} [22], weakening the temperature differential between the opposing water masses and allowing a north-eastward intrusion of Atlantic waters into the

Barents Sea [107]. The fact that changes in species activity and behaviour that affect important aspects of the ecosystem (nutrient concentrations) are maximized at the frontal edge, and that this boundary represents a distinction (high south–low north) in faunal mediation capacity, highlights the significance of this boundary for defining functional precincts and ecological boundaries [30]. Changes in species and functional groups between seasons, attributed to the presence of more labile organic matter reaching the seafloor in summer, provide anecdotal support for this assertion [64]. Indeed, recent work has shown that such spatial-temporal changes are linked to the functional traits of organisms because environmental context—in particular sea ice and bottom water temperature [35]—influences the trait expression of individuals which, in turn, dictates net community-level behaviour and ecosystem functioning [99,108]. Comparison of our northern and southern faunal clusters provide some insight as to what may lie in store (elevated bioturbation and nutrients) as organisms adapted to seasonally ice-covered Arctic shelf habitats are replaced (local extinction) by southern Atlantic species, but it would be naïve to assume that this transition in faunal composition will define ecosystem functioning. As evidenced here, a change or rearrangement in the absolute contributions that species make to ecosystem process and function can be influential [109], even when a single species (here, the amphipod *Quasimelita quadrispinosa*) with poor numeric or biomass representation dominates the functional return [110,111]. Such instances may arise from resource, competitive or predation release, and may be localized and short-lived in duration, but may act to prevent functional homogenization across the region [112]. Information on the role of individual species, species-environment interactions and interspecies relations in modifying ecosystem processes and functioning is woefully inadequate for the Arctic benthos [78], often inferred or generalized [29], and lacks empirical support.

Whether climate-driven changes in the functional architecture of communities lead to the decline, maintenance or enhancement of ecosystem functioning will not only depend on the level of functional redundancy across multiple supporting processes [113,114] but also on the environmental circumstances under which faunal reorganization take place. As there is a strong coupling between export flux, including episodic events of sinking ice algae aggregates [115], community structure [116] and benthic carbon cycling [117], it follows that complex dependencies between trait composition and the timing and quality of organic matter are likely. A significant feature of our study was the dramatic contrast in ice cover between years, which we assume will have changed the timing of the primary production regime and the way in which energy and nutrients transit through the food web [11,31]. In 2018, the reduction in sea ice extent prompted an earlier phytoplankton bloom relative to the previous year, such that organic matter reaching the seafloor will have been degraded through grazing in 2018 and comprised fresh material in 2017 [53,118]. Comparison of the consecutive summers in our study suggests that there is greater reworking of the sediment-water interface and deeper mixing of the sediment profile under conditions of advanced ice retreat, as well as a more pronounced contrast in activity between southern and northern communities, although we do recognize that spatial and temporal variability may override this signal under certain circumstances [40,72]. Hence, our findings indicate that bioturbation activity is dependent on the interactive effects of season and sea ice condition which, in turn, are influenced by latitudinal position and local adjustments to circumstance. Furthermore, since the inventory of sediment organic material indicates more efficient carbon processing (lower organic material values) during extended sea ice conditions [73], the increased reworking activities of infauna during these periods may offer a mechanistic explanation for likely/potential greater carbon burial rates, at least at the most northerly stations in the transect [53]. If true, interspecific differences in community bioturbation should lead to variations in the vertical distribution of sediment organic matter, a conclusion that does appear to be consistent with observations of organic material profiles [72] and other sediment processes (Fe/Mn reduction, [119]). Direct links between aerobic processes, reactive organic carbon and highest abundances of bacteria and archaea have recently been shown for the uppermost sediment layers, and organic matter reactivity changes most dramatically at, and directly below, the sediment-water interface alongside sedimentology and biological activity [73]. However, invertebrate utilization of carbon can occur at the biochemical level [120] and/or

depend on species-specific differences in adsorption efficiency and feeding behaviour [121], suggesting that multiple traits that each interact with climatic forcing will be important for resource exploitation and ecosystem functioning.

5. Conclusion

We have demonstrated the importance of seasonal timing (here, the onset of summer) and context in moderating how benthic communities respond to external forcing that might help explain any departure from expectations based on latitudinal position in relation to macroclimatic drivers of change. It is clear that species alter their activity and/or functional role under different environmental conditions and that complex dependencies are likely to occur between community composition and the timing and quality of organic matter which, in turn, would govern the faunal mediation of ecosystem functioning. We anticipate, however, that spatial and temporal variability in environmental setting will be important in explaining biodiversity-functioning relations at larger scales [40], and may be more important than localized changes in sea ice [72] and its correlates. Our study also highlights the paucity of available information within this region on how species (or communities) moderate important ecosystem functions in relation to a changing climate, biotic re-organization, and their interactions with one another [70]. Furthermore, biogeochemical pathways and processes are poorly understood, and little is known about the relative importance of different components of organic material at an ecosystem level [73,122]. In order to establish generality and generate projections of the threats and opportunities of future change on biological and biogeochemical processes, process and experimental studies focused on developing mechanistic understanding of the interactive effects of different components of change (and any of their correlates) on organism-sediment relations are urgently needed and must be prioritized.

References

1. Kedra M *et al.* 2015 Status and trends in the structure of Arctic benthic food webs. *Polar Res.* **34**, 23775. (doi:10.3402/polar.v34.23775)
2. Drinkwater KF. 2011 The influence of climate variability and change on the ecosystems of the Barents Sea and adjacent waters: review and synthesis of recent studies from the NESSAS Project. *Progr. Oceanogr.* **90**, 47–61. (doi:10.1016/j.pocean.2011.02.006)
3. Burrows MT *et al.* 2011 The pace of shifting climate in marine and terrestrial ecosystems. *Science* **334**, 652–655. (doi:10.1126/science.1210288)

4. Wallhead PJ, Bellerby RGJ, Silyakova A, Slagstad D, Polukhin AA. 2017 Bottom water acidification and warming on the Western Eurasian Arctic shelves: dynamical downscaling projections. *J. Geophys. Res.* **122**, 8126–8144. (doi:10.1002/2017JC013231)

5. Beaugrand G *et al.* 2019 Prediction of unprecedented biological shifts in the global ocean. *Nat. Clim. Change* **9**, 237–343. (doi:10.1038/s41558-019-0420-1)

6. Degen R, Jorgensen LL, Ljubin P, Ellingsen IH, Pehlke H, Brey T. 2016 Patterns and drivers of megabenthic secondary production on the Barents Sea shelf. *Mar. Ecol. Progr. Ser.* **546**, 1–16. (doi:10.3354/meps11662)

7. Waga H, Hirawake T, Grebmeier JM. 2020 Recent change in benthic macrofaunal community composition in relation to physical forcing in the Pacific Arctic. *Polar Biol.* **43**, 285–294. (doi:10.1007/s00300-020-02632-3)

8. Kedra M, Cooper LW, Zhangb M, Biasattib D, Grebmeierb JM. 2019 Benthic trophic sensitivity to on-going changes in Pacific Arctic seasonal sea ice cover – Insights from the nitrogen isotopic composition of amino acids. *Deep-Sea Res. II* **162**, 137–151. (doi:10.1016/j.dsr2.2019.01.002)

9. Brault EK, Koch PL, McMahon KW, Broach KH, Rosenfield AP, Sauthoff W, Loeb VJ, Arrigo KR, Smith WO. 2018 Carbon and nitrogen zooplankton isoscapes in West Antarctica reflect oceanographic transitions. *Mar. Ecol. Progr. Ser.* **593**, 29–45**.** (doi:10.3354/meps12524)

10. Tuomi M, Stark S, Hoset KS, Vaisanen M, Oksanen L, Murguzur FJA, Tuomisto H, Dahlgren J, Brathen KA. 2019 Herbivore effects on ecosystem process rates in a low-productive system. *Ecosystems* **22**, 827–843. (doi:10.1007/s10021-018-0307-4)

11. Leu E, Soreide JE, Hessen DO, Falk-Petersen S, Berge J. 2011 Consequences of changing sea-ice cover for primary and secondary producers in the European Arctic shelf seas: timing, quantity, and quality. *Prog. Oceanogr.* **90**, 18–32. (doi:10.1016/j.pocean.2011.02.004)

12. Boetius A *et al.* 2013 Export of algal biomass from the melting Arctic sea ice. *Science* **339**, 1430–1432. (doi:10.1126/science.1231346)

13. Bridier G, Meziane T, Grall J, Chauvaud L, Sejr M, Menneteau S, Olivier F. 2019 Coastal waters freshening and extreme seasonality affect organic matter sources, quality, and transfers in a High Arctic fjord (Young Sound, Greenland). *Mar. Ecol. Progr. Ser.* **610**, 15–31. (doi:10.3354/meps12857)

14. Underwood GJC, Michel C, Meisterhans G, Niemi A, Belzile C, Witt M, Dumbrell AJ, Koch BP. 2019 Organic matter from Arctic sea-ice loss alters bacterial community structure and function. *Nat. Clim. Change* **9**, 170–176. (doi:10.1038/s41558-018-0391-7)

15. Post E. 2017 Implications of earlier sea ice melt for phenological cascades in arctic marine food webs. *Food Webs* **13**, 60–66. (doi:10.1016/j.fooweb.2016.11.002)

16. Kass M, Vedenin A, Hasemann C, Brandt A, Soltwedel T. 2019 Community structure of macrofauna in the deep Fram strait: a comparison between two bathymetric gradients in ice-covered and ice-free areas. *Deep Sea Res. I* **152**, 103102. (doi:10.1016/j.dsr.2019.103102)

17. Rybakova E, Kremenetskaia A, Vedenin A, Boetius A, Gebruk A. 2019 Deep-sea megabenthos communities of the Eurasian Central Arctic are influenced by ice-cover and sea-ice algal falls. *PLoS ONE* **14**, e0211009. (doi:10.1371/journal.pone.0211009)

18. McTigue ND, Gardner WS, Dunton KH, Hardison AK. 2016 Biotic and abiotic controls on co-occurring nitrogen cycling processes in shallow Arctic shelf sediments. *Nat. Commun.* **7**, 13145. (doi:10.1038/ncomms13145)

19. Hoffmann R, Braeckman U, Hasemann C, Wenzhöfer F. 2018 Deep-sea benthic communities and oxygen fluxes in the Arctic Fram Strait controlled by sea-ice cover and water depth. *Biogeosciences* **15**, 4849–4869. (doi:10.5194/bg-15-4849-2018)

20. Barton BI, Lenn Y-D, Lique C. 2018 Observed Atlantification of the Barents Sea causes the Polar Front to limit the expansion of winter sea ice. *J. Phys. Oceanogr.* **48**, 1849–1866. (doi:10.1175/JPO-D-18-0003.1)

21. Lind S, Ingvaldsen RB, Furevik T. 2018 Arctic warming hotspot in the northern Barents Sea linked to declining sea-ice import. *Nat. Clim. Change* **8**, 634–639. (doi:10.1038/s41558-018-0205-y)

22. Neukermans G, Oziel L, Babin M. 2018 Increased intrusion of warming Atlantic water leads to rapid expansion of temperate phytoplankton in the Arctic. *Glob. Change Biol.* **24**, 2545–2553. (doi:10.1111/gcb.14075)

23. Vihtakari M, Welcker J, Moe B, Chastel O, Tartu S, Hop H, Bech C, Descamps S, Gabrielsen GW. 2018 Black-legged kittiwakes as messengers of Atlantification in the Arctic. *Sci. Rep.* **8**, 1178. (doi:10.1038/s41598-017-19118-8)

24. Grabowski M, Jablonska A, Weydmann-Zwolicka A, Gantsevich M, Strelkov P, Skazina M, Weslawski JM. 2019 Contrasting molecular diversity and demography patterns in two intertidal amphipod crustaceans reflect Atlantification of High Arctic. *Mar. Biol.* **166**, 155. (doi:10.1007/s00227-019-3603-4)

25. Golikov AV, Sabirov RM, Lubin PA, Jørgensen LL. 2013 Changes in distribution and range structure of Arctic cephalopods due to climatic changes of the last decades. *Biodiversity* **14**, 28–35. (doi:10.1080/14888386.2012.702301)

26. Fossheim M, Primicerio R, Johannessen E, Ingvaldsen RB, Aschan MM, Dolgov AD. 2015 Recent warming leads to a rapid borealization of fish communities in the Arctic. *Nat. Clim. Change* **5**, 673–677. (doi:10.1038/NCLIMATE2647)

27. Grebmeier JM, Frey KE, Cooper LW, Kedra M. 2018 Trends in benthic macrofaunal populations, seasonal sea ice persistence, and bottom water temperatures in the Bering Strait region. *Oceanography* **31**, 136–151. (doi:10.5670/oceanog.2018.224)

28. Cochrane SKJ, Pearson TH, Greenacre M, Costelloe J, Ellingsen IH, Dahle S, Gulliksen B. 2012 Benthic fauna and functional traits along a Polar Front transect in the Barents Sea – advancing tools for ecosystem-scale assessments. *J. Mar. Syst.* **94**, 204–217. (doi:10.1016/j.jmarsys.2011.12.001)

29. Degen R, Faulwetter S. 2019 The Arctic Traits Database – a repository of Arctic benthic invertebrate traits. *Earth Syst. Sci. Data* **11**, 301–322. (doi:10.5194/essd-11-301-2019)

30. Kun L *et al.* 2019 Functional trait composition and diversity patterns of marine macrobenthos across the Arctic Bering Sea. *Ecol. Ind.* **102**, 673–685. (doi:10.1016/j.ecolind.2019.03.029)

31. Reigstad M, Carroll J, Slagstad D, Ellingsen I, Wassmann P. 2011 Intra-regional comparison of productivity, carbon flux and ecosystem composition within the northern Barents Sea. *Prog. Oceanogr.* **90**, 33–64. (doi:10.1016/j.pocean.2011.02.005)

32. Cavalieri DJ, Parkinson CL. 2012 Arctic sea ice variability and trends, 1979–2010. *Cryposphere* **6**, 881–889. (doi:10.5194/tc-6-881-2012)

33. Drinkwater, KF, Kristiansen, T. 2018 A synthesis of the ecosystem responses to the late 20th century cold period in the northern North Atlantic. *ICES J. Mar. Sci.* **75**, 2325–2341. (doi:10.1093/icesjms/fsy077)

34. Kortsch S, Primicerio R, Beuchel F, Renaud PE, Rodrigues J, Lønne OJ, Gulliksen B. 2012 Climate-driven regime shifts in Arctic marine benthos. *Proc. Natl Acad. Sci. USA* **109**, 14 052–14 057. (doi:10.1073/pnas.1207509109)

35. Frainer A, Primicerio R, Kortsch S, Aune M, Dolgov AV, Fossheim M, Aschan MM. 2017 Climate-driven changes in functional biogeography of Arctic marine fish communities. *Proc. Natl Acad. Sci. USA* **114**, 12 202–12 207. (doi:10.1073/pnas.1706080114)

36. Sirenko BI, Gagaev SY. 2007 Unusual abundance of macrobenthos and biological invasions in the Chukchi Sea. *Russ. J. Mar. Biol.* **33**, 355–364. (doi:10.1134/S1063074007060016)

37. Gauzens B, Rall BC, Mendonça V, Vinagre C, Brose U. 2020 Biodiversity of intertidal food webs in response to warming across latitudes. *Nat. Clim. Change* **10**, 264–269. (doi:10.1038/s41558-020-0698-z)

38. Griffith GP, Hop H, Vihtakari M, Wold A, Kalhagen K, Gabrielsen GW. 2019 Ecological resilience of Arctic marine food webs to climate change. *Nat. Clim. Change* **9**, 868–872. (doi:10.1038/s41558-019-0601-y)

39. Godbold JA, Solan M. 2013 Long-term effects of warming and ocean acidification are modified by seasonal variation in species responses and environmental conditions. *Phil. Tran. R. Soc. B* **368**, 20130186. (doi:10.1098/rstb.2013.0186)

40. Wohlgemuth D, Solan M, Godbold JA. 2017 Species contributions to ecosystem process and function can be population dependent and modified by biotic and abiotic setting. *Proc. R. Soc. B* **284**, 20162805. (doi:10.1098/rspb.2016.2805)

41. Thomsen MS, Garcia C, Bolam SG, Parker R, Godbold JA, Solan M. 2017 Consequences of biodiversity loss diverge from expectation due to post-extinction compensatory responses. *Sci. Rep.* **7**, 43695. (doi:10.1038/srep43695)

42. Koltz AM, Schmidt NM, Høye TT. 2018 Differential arthropod responses to warming are altering the structure of Arctic communities. *R. Soc. Open Sci.* **5**, 171503. (doi:10.1098/rsos.171503)

43. Snelgrove PVR *et al.* 2018 Global carbon cycling on a heterogeneous seafloor. *Trends Ecol. Evol.* **33**, 96–105. (doi:10.1016/j.tree.2017.11.004)

44. Levin LN, Blair N, DeMaster D, Plaia G, Fornes W, Martin C, Thomas C. 1997 Rapid subduction of organic matter by maldanid polychaetes on the North Carolina slope. *J. Mar. Res.* **55**, 595–611. (doi:10.1357/0022240973224337)

45. Josefson AB, Forbes TL, Rosenberg R. 2002 Fate of phytodetritus in marine sediments: functional importance of macrofaunal community. *Mar. Ecol. Prog. Ser.* **230**, 71–85. (doi:10.3354/meps230071)

46. Aller RC. 1982 The effects of macrobenthos on chemical properties of marine sediment and overlying water. In *Animal–sediment relations—The biogenic alteration of sediments* (eds PL McCall, MJS Tevesz), pp. 53–102. New York, NY: Plenum Press.

47. Kristensen E, Delefosse M, Quintana CO, Flindt MR, Valdemarsen T. 2014 Influence of benthic macrofauna community shifts on ecosystem functioning in shallow estuaries. *Front. Mar. Sci.* **1**, 41. (doi:10.3389/fmars.2014.00041)

48. Grossi V, Caradec S, Gilbert F. 2003 Burial and reactivity of sedimentary microalgal lipids in bioturbated Mediterranean coastal sediments. *Mar. Chem.* **81**, 57–69. (doi:10.1016/S0304-4203(02)00139-1)

49. Aller RC. 1994 Bioturbation and remineralization of sedimentary organic matter: effects of redox oscillation. *Chem. Geol.* **114**, 331–345. (doi:10.1016/0009-2541(94)90062-0)

50. Schluter M, Sauter E, Hansen HP, Suess E. 2000 Seasonal variations of bioirrigation in coastal sediments: modelling of field data. *Geochem. Cosmochim. Acta* **64**, 821–834. (doi:10.1016/S0016-7037(99)00375-0)

51. Bourgeois S, Archambault P, Witte U. 2017 Organic matter remineralization in marine sediments: a Pan-Arctic synthesis. *Global Biogeochem. Cycles* **31**, 190–213. (doi:10.1002/2016GB005378)

52. Smith C, DeMaster D, Thomas C, Srsen P, Grange L, Evrard V, DeLeo F. 2012 Pelagic-benthic coupling, food banks, and climate change on the West Antarctic Peninsula Shelf. *Oceanography* **25**, 188–201. (doi:10.5670/oceanog.2012.94)

53. Stevenson MA, Abbott GD. 2019 Exploring the composition of macromolecular organic matter in Arctic Ocean sediments under a changing sea ice gradient. *J. Analyt. Appl. Pyrolysis* **140**, 102–111. (doi:10.1016/j.jaap.2019.02.006)

54. Clough LM, Ambrose Jr WG, Cochran JK, Barnes C, Renaud PE, Aller RC. 1997 Infaunal density, biomass and bioturbation in the sediments of the Arctic Ocean. *Deep-Sea Res. II* **44**, 1683–1704. (doi:10.1016/S0967-0645(97)00052-0)

55. Middelburg JJ. 2018 Reviews and syntheses: to the bottom of carbon processing at the seafloor. *Biogeosciences* **15**, 413–427. (doi:10.5194/bg-15-413-2018)

56. Jørgensen LL, Ljubin P, Skjoldal HR, Ingvaldsen RB, Anisimova N, Manushin I. 2015 Distribution of benthic megafauna in the Barents Sea: baseline for an ecosystem approach to management. *ICES J. Mar. Sci.* **72**, 595–613. (doi:10.1093/icesjms/fsu106)

57. Lacharité M, Jørgensen LL, Metaxas A, Lien VS, Skjoldal HR. 2016 Delimiting oceanographic provinces to determine drivers of mesoscale patterns in benthic megafauna: a case study in the Barents Sea. *Prog. Oceanogr.* **146**, 187–198. (doi:10.1016/j.pocean.2016.06.008)

58. Buhl-Mortensen P, Dolan MFJ, Ross RE, Gonzalez-Mirelis G, Buhl-Mortensen L, Bjarnadóttir LR, Albretsen J. 2020 Classification and mapping of benthic biotopes in Arctic and Sub-Arctic Norwegian waters. *Front. Mar. Sci.* **7**, 271. (doi:10.3389/fmars.2020.00271)

59. Link H, Chaillou G, Forest A, Piepenburg D, Archambault P. 2013 Multivariate benthic ecosystem functioning in the Arctic – benthic fluxes explained by environmental parameters in the southeastern Beaufort Sea. *Biogeosciences* **10**, 5911–5929. (doi:10.5194/bg-10-5911-2013)

60. Carroll J, Zaborska A, Papucci C, Schirone A, Carroll ML, Pempkowiak J. 2008 Accumulation of organic carbon in western Barents Sea sediments. *Deep Sea Res. II* **55**, 2361–2371. (doi:10.1016/j.dsr2.2008.05.005)

61. Maiti K, Carroll J, Benitez-Nelson CR. 2010 Sedimentation and particle dynamics in the seasonal ice zone of the Barents Sea. *J. Mar. Syst.* **79**, 185–198. (doi:10.1016/j.jmarsys.2009.09.001)

62. Morata N, Michaud E, Włodarska-Kowalczuk M. 2013 Impact of early food input on the Arctic benthos activities during the polar night. *Polar Biol.* **38**, 99–114. (doi:10.1007/s00300-013-1414-5)

63. Petrowski S, Molis M, Schachtl K, Buschbaum C. 2015 Do bioturbation and consumption affect coastal Arctic marine soft-bottom communities? *Polar Biol.* **39**, 2141–2153. (doi:10.1007/s00300-015-1654-7)

64. Oleszczuk B, Michaud E, Morata N, Renaud PE, Kędra M. 2019 Benthic macrofaunal bioturbation activities from shelf to deep basin in spring to summer transition in the Arctic Ocean. *Mar. Environ. Res.* **150**, 104746. (doi:10.1016/j.marenvres.2019.06.008)

65. Soltwedel T, Hasemann C, Vedenin A, Bergmann M, Taylor J, Krauß F. 2019 Bioturbation rates in the deep Fram Strait: results from *in situ* experiments at the arctic LTER observatory HAUSGARTEN. *J. Exp. Mar. Biol. Ecol.* **511**, 1–9. (doi:10.1016/j.jembe.2018.11.001)

66. Loeng H. 1991 Features of the physical oceanographic conditions of the Barents Sea. *Polar Res.* **10**, 5–18. (doi:10.1111/j.1751-8369.1991.tb00630.x)

67. Erga SR, Ssebiyonga N, Hamre B, Frette O, Rey F, Drinkwater K. 2014 Nutrients and phytoplankton biomass distribution and activity at the Barents Sea Polar Front during summer near Hopen and Storbanken. *J. Mar. Syst.* **130**, 181–192. (doi:10.1016/j.jmarsys.2012.12.008)

68. Sweetman AK *et al.* 2017 Major impacts of climate change on deep-sea benthic ecosystems. *Elem. Sci. Anth.* **5**, 4. (doi:10.1525/elementa.203)

69. Misund OA, Heggland K, Skogseth R, Falck E, Gjøsæter H, Sundet J, Watne J, Lønne OJ. 2016 Norwegian fisheries in the Svalbard zone since 1980. Regulations, profitability and warming waters affect landings. *Polar Sci.* **10**, 312–322. (doi:10.1016/j.polar.2016.02.001)

70. Jørgensen LL, Primicerio R, Ingvaldsen RB, Fossheim M, Strelkova N, Thangstad TH, Manushin I, Zakharov D. 2019 Impact of multiple stressors on sea bed fauna in a warming Arctic. *Mar. Ecol. Prog. Ser.* **608**, 1–12. (doi:10.3354/meps12803)

71. Souster TA, Barnes DKA, Hopkins J. 2020 Variation in zoobenthic blue carbon in the Arctic's Barents Sea shelf sediments. *Phil. Trans. R. Soc. A* **378**, 20190362. (doi:10.1098/rsta.2019.0362)

72. Freitas FS, Hendry KR, Henley SF, Faust JC, Tessin AC, Stevenson MA, Abbott GD, März C, Arndt S. 2020 Benthic-pelagic coupling in the Barents Sea: an integrated data-model framework. *Phil. Trans. R. Soc. A* **378**, 20190359. (doi:10.1098/rsta.2019.0359)

73. Stevenson MA *et al.* 2020 Transformation of organic matter in a Barents Sea sediment profile: coupled geochemical and microbiological processes. *Phil. Trans. R. Soc. A* **378**, 20200223. (doi:10.1098/rsta.2020.0223)

74. Folk RL. 1974 *Petrology of sedimentary rocks*, 170pp. Austin, TX: Hemphill Publishing.

75. Blott SJ, Pye K. 2001 GRADISTAT: a grain size distribution and statistics package for the analysis of unconsolidated sediments. *Earth Surf. Processes Landforms* **26**, 1237–1248. (doi:10.1002/esp.261)

76. Solan M, Wigham BD, Hudson IR, Kennedy R, Coulon CH, Norling K, Nilsson HC, Rosenberg R. 2004 In situ quantification of bioturbation using time-lapse fluorescent sediment profile imaging (f-SPI), luminophore tracers and model simulation. *Mar. Ecol. Progr. Ser.* **271**, 1–12. (doi:10.3354/meps271001)

77. Schiffers K, Teal LR, Travis JMJ, Solan M. 2011 An open source simulation model for soil and sediment bioturbation. *PLoS ONE* **6**, e28028. (doi:10.1371/journal.pone.0028028)

78. Solan M, Ward ER, White EL, Hibberd EE, Cassidy C, Schuster JM, Hale R, Godbold JA. 2019 Worldwide measurements of bioturbation intensity, ventilation rate, and the mixing depth of marine sediments. *Sci. Data* **6**, 58. (doi:10.1038/s41597-019-0069-7)

79. Crank J. 1975 *The mathematics of diffusion*. Oxford, UK: Oxford University Press.

80. Forster S, Glud RN, Gundersen JK, Huettel M. 1999 *In situ* study of bromide tracer and oxygen flux in coastal sediment. *Estuar. Coast Shelf Sci.* **49**, 813–827. (doi:10.1006/ecss.1999.0557)

81. Rumohr H. 1990 *Soft bottom macrofauna: collection and treatment of samples. ICES, techniques in marine environmental sciences, No. 8*. Copenhagen: ICES.

82. Zuur AF, Ieno EN, Elphick CS. 2010 A protocol for data exploration to avoid common statistical problems. *Methods Ecol. Evol.* **1**, 3–14. (doi:10.1111/j.2041-210X.2009.00001.x)

83. Pinheiro JC, Bates DM. 2000 *Mixed effects models in S and S-plus*. New York, NY; Berlin, Germany: Springer.

84. West BT, Welch KB, Gatecki AT. 2007 *Linear mixed models. A practical guide using statistical*

16

royalsocietypublishing.org/journal/rsta   *Phil. Trans. R. Soc. A* **378**: 20190365

software. London, UK: Chapman and Hall.

85. Diggle PJ, Heagerty P, Liang KY, Zeger SL. 2002 *Analysis of longitudinal data*. Oxford, UK: Oxford University Press.

86. Anderson MJ. 2001 A new method for non-parametric multivariate analysis of variance. *Austr. Ecol.* **26**, 32–46. (doi:10.1111/j.1442-9993.2001.01070.pp.x)

87. Clarke KR. 1993 Non-parametric multivariate analyses of changes in community structure. *Austr. J. Ecol.* **18**, 117–143. (doi:10.1111/j.1442-9993.1993.tb00438.x)

88. Clarke KR, Somerfield PJ, Chapman MG 2006 On resemblance measures for ecological studies. Including taxonomic dissimilarities and a zero-adjusted Bray-Curtis coefficient for denuded assemblages. *J. Exp. Mar. Biol. Ecol.* **330**, 55–80. (doi:10.1016/j.jembe.2005.12.017)

89. R Core Team. 2018 *R: A language and environment for statistical computing*. Vienna, Austria: R Foundation for Statistical Computing. See http://www.R-project.org/.

90. Pinheiro J, Bates D. 2018 nlme: linear and nonlinear mixed effects models. R package version 3.1–137. See http://cran.r-project.org/web/packages/nlme/index.html.

91. Oksanen J *et al.* 2019 Community ecology package 2.5–6. See http://cran.r-project.org/web/packages/vegan/index.html.

92. Cardinale BJ *et al.* 2012 Biodiversity loss and its impact on humanity. *Nature* **486**, 59–67. (doi:10.1038/nature11148)

93. Huntington HP *et al.* 2020 Evidence suggests potential transformation of the Pacific Arctic ecosystem is underway. *Nat. Clim. Change* **10**, 342–348. (doi:10.1038/s41558-020-0695-2)

94. Rillig MC, Ryo M, Lehmann A, Aguilar-Trigueros CA, Buchert S, Wulf A, Iwasaki A, Roy J, Yang GW. 2019 The role of multiple global change factors in driving soil functions and microbial biodiversity. *Science* **366**, 886–890. (doi:10.1126/science.aay2832)

95. Zellweger F *et al.* 2020 Forest microclimate dynamics drive plant responses to warming. *Science* **368**, 772–775. (doi:10.1126/science.aba6880)

96. Pennekamp F *et al.* 2018 Biodiversity increases and decreases ecosystem stability. *Nature* **563**, 109–114. (doi:10.1038/s41586-018-0627-8)

97. Bulling MT, Solan M, Dyson KE, Hernandez-Milian G, Luque P, Pierce GJ, Raffaelli D, Paterson DM, White PCL. 2008 Species effects on ecosystem processes are modified by faunal responses to habitat composition. *Oecologia* **158**, 511–520. (doi:10.1007/s00442-008-1160-5)

98. Hiddink JG, Davies TW, Perkins M, Machairopoulou M, Neill SP. 2009 Context dependency of relationships between biodiversity and ecosystem functioning is different for multiple ecosystem functions. *Oikos* **118**, 1892–1900. (doi:10.1111/j.1600-0706.2009.17556.x)

99. Cassidy C, Grange LJ, Garcia C, Bolam SG, Godbold JA. 2020 Species interactions and environmental context affect intraspecific behavioural trait variation and ecosystem function. *Proc. R. Soc. B* **287**, 20192143. (doi:10.1098/rspb.2019.2143)

100. Renaud PE, Wallhead P, Kotta J, Wtodarska-Kowalczuk M, Bellerby RGJ, Ratsep M, Slagstad D, Kuklinski P. 2019 Arctic sensitivity? Suitable habitat for benthic taxa is surprisingly robust to climate change. *Front. Mar. Sci.* **6**, 538. (doi:10.3389/fmars.2019.00538)

101. McClain CR, Webb TJ, Nunnally CC, Dixon SR, Finnegan S, Nelson JA. 2020 Metabolic niches and biodiversity: a test case in the deep sea benthos. *Front. Mar. Sci.* **7**, 216. (doi:10.3389/fmars.2020.00216)

102. Hale R, Godbold JA, Sciberras M, Dwight J, Wood C, Hiddink JG, Solan M. 2017 Mediation of macronutrients and carbon by post-disturbance shelf sea sediment communities. *Biogeochemistry* **135**, 121–133. (doi:10.1007/s10533-017-0350-9)

103. Ohlsson M, Eklöf A. 2020 Spatial resolution and location impact group structure in a marine food web. *Ecol. Lett.* (doi:10.1111/ele.13567)

104. Oziel L, Sirven J, Gascard J-C. 2016 The Barents Sea frontal zones and water masses variability (1980–2011). *Ocean Sci.* **12**, 169–184. (doi:10.5194/os-12-169-2016)

105. Oziel L, Neukermans G, Ardyna M, Lancelot C, Tison J-L, Wassmann P, Sirven J, Ruiz-Pino D, Gascard J-C. 2017 Role for Atlantic inflows and sea ice loss on shifting phytoplankton blooms in the Barents Sea. *J. Geophys. Res.* **122**, 5121–5139. (doi:10.1002/2016jc012582)

106. Zaporozhtsev I, Moiseev D. 2018 Calculation of Atlantic Waters Inflow and Polar Front Position in the Barents Sea with Long-Term Data on Kola Transect. In *2018 4th Int. Symp. on Geoinformatics (ISyG)*, *IEEE*.

107. Lind S, Ingvaldsen RB. 2012 Variability and impacts of Atlantic Water entering the Barents Sea from the north. *Deep Sea Res. I* **62**, 70–88. (doi:10.1016/j.dsr.2011.12.007)

108. Dolbeth M, Crespo D, Leston S, Solan M. 2019 Realistic scenarios of environmental

disturbance lead to functionally important changes in benthic species-environment interactions. *Mar. Environ. Res.* **150**, 104770. (doi:10.1016/j.marenvres.2019.104770)

109. Wohlgemuth D, Solan M, Godbold JA. 2016 Specific arrangements of species dominance can be more influential than evenness in maintaining ecosystem process and function. *Sci. Rep.* **6**, 39325. (doi:10.1038/srep39325)

110. Solan M, Cardinale BJ, Downing AL, Engelhardt KAM, Ruesink JL, Srivastava DS 2004 Extinction and ecosystem function in the marine benthos. *Science* **306**, 1177–1180. (doi:10.1126/science.1103960)

111. Henderson CJ *et al.* 2020 Low redundancy and complementarity shape ecosystem functioning in a low-diversity ecosystem. *J. Anim. Ecol.* **89**, 784–794. (doi:10.1111/1365-2656.13148)

112. Lindholm M, Alahuhta J, Heino J, Hjort, J, Toivonen H. 2020 Changes in the functional features of macrophyte communities and driving factors across a 70-year period. *Hydrobiologia* (doi:10.1007/s10750-019-04165-1)

113. Aune M, Aschan MM, Greenacre M, Dolgov AV, Fossheim M, Primicerio R. 2018 Functional roles and redundancy of demersal Barents Sea fish: ecological implications of environmental change. *PLoS ONE* **13**, e0207451. (doi:10.1371/journal.pone.0207451)

114. Pessarrodona A, Foggo A, Smale DA. 2019 Can ecosystem functioning be maintained despite climate-driven shifts in species composition? Insights from novel marine forests. *J. Ecol.* **107**, 91–104. (doi:10.1111/1365-2745.13053)

115. Wiedmann I, Ershova E, Bluhm BA, Nöthig E-M, Gradinger RR, Kosobokova K, Boetius A. 2020 What feeds the benthos in the Arctic Basins? Assembling a carbon budget for the deep Arctic Ocean. *Front. Mar. Sci.* **7**, 224. (doi:10.3389/fmars.2020.00224)

116. Lovvorn JR, North CA, Grebmeier JM, Cooper LW, Kolts JM. 2018 Sediment organic carbon integrates changing environmental conditions to predict benthic assemblages in shallow Arctic seas. *Aquatic Conserv.* **28**, 861–871. (doi:10.1002/aqc.2906)

117. Renaud PE, Morata N, Carroll ML, Denisenko SG, Reigstad M. 2008 Pelagic–benthic coupling in the western Barents Sea: processes and time scales. *Deep Sea Res. II* **55**, 2372–2380. (doi:10.1016/j.dsr2.2008.05.017)

118. Morata N, Renaud PE. 2008 Sedimentary pigments in the western Barents Sea: a reflection of pelagic–benthic coupling? *Deep Sea Res. II* **55**, 2381–2389. (doi:10.1016/j.dsr2.2008.05.004)

119. Nickel M, Vandieken V, Brüchert V, Jørgensen BB. 2008 Microbial Mn(IV) and Fe(III) reduction in northern Barents Sea sediments under different conditions of ice cover and organic carbon deposition. *Deep Sea Res. II* **55**, 2390–2398. (doi:10.1016/j.dsr2.2008.05.003)

120. Howell KL, Pond DW, Billet DSM, Tyler PA.2003 Feeding ecology of deep-sea seastars (Echinodermata: Asteroidea): a fatty-acid biomarker approach. *Mar. Ecol. Prog. Ser.* **255**, 193–206. (doi:10.3354/meps255193)

121. Godbold JA, Rosenberg R, Solan M. 2009 Species-specific traits rather than resource partitioning mediate diversity effects on resource use. *PLoS ONE* **4**, e7423. (doi:10.1371/journal.pone.0007423)

122. Rossel PE, Bienhold C, Hehemann L, Dittmar T, Boetius A. 2020 Molecular composition of dissolved organic matter in sediment porewater of the Arctic deep-sea observatory HAUSGARTEN (Fram Strait). *Front. Mar. Sci.* **7**, 428. (doi:10.3389/fmars.2020.00428)